Journal of Manufacturing Processes 18 (2015) 131–140

Contents lists available at ScienceDirect

Journal of Manufacturing Processes

journal homepage: www.elsevier.com/locate/manpro

Technical Paper

Numerical and experimental investigations of hydro-mechanical deep drawing process of laminated aluminum/steel sheets

S. Bagherzadeh[a,*], M.J. Mirnia[b], B. Mollaei Dariani[c]

[a] Department of Mechanical Engineering, College of Engineering, University of Tehran, Tehran, Iran
[b] Department of Mechanical Engineering, Babol Noshirvani University of Technology, Babol, Iran
[c] Department of Mechanical Engineering, Amirkabir University of Technology, Tehran, Iran

ARTICLE INFO

Article history:
Received 15 December 2014
Received in revised form 7 March 2015
Accepted 8 March 2015
Available online 27 March 2015

Keywords:
HMDD
Laminated sheet
FE simulation
Formability
Process window
Lay-up

ABSTRACT

The application of hydro-mechanical deep drawing (HMDD) process on laminated sheets combines advantages of both process and material to improve the forming condition of poor formable light-weight metals such as aluminum alloys. In this research, the HMDD process of anisotropic laminated bimetallic sheets has been analyzed using a 3D finite element simulation with implementing Fortran based code for accurate modeling of non-uniform oil pressure distribution. To verify FE results, experimental works were conducted on the widely used laminated aluminum/steel sheets. Based on the developed FE model, parametric studies were performed to investigate the effect of material parameters such as layers thickness and lay-up arrangement on the forming condition, process window and formability of aluminum sheet as key process parameters. Results demonstrated that suitable process condition to attain a successful forming of bimetallic aluminum/steel sheets can be predicted by developed FE model reasonably. Also, It shown that wider working zone was achievable with decrease in drawing ratio, reduction in thickness of sheet with lower strength layer and also when aluminum sheet is in contact with punch (A/S lay-up). In addition, the higher limiting drawing ratio (LDR) and lower thinning in low formable aluminum sheet would be achievable in A/S lay-up than S/A lay-up.

1. Introduction

Application of laminated structures and components made of sheet metals with mismatch materials has been developed primarily because of making various combined mechanical, physical, and chemical properties by the base materials. Laminated metal sheets can be fabricated using different joining methods such as explosive welding, roll bonding and adhesive bonding. Among, two-layer composite sheets manufactured by roll bonding composed of one layer with appropriate strength and a good corrosion resistance, wear resistance, or electrical conductivity of the other layer, have found wide applications in chemical, electrical, ship, food and building industries [1].

In recent years, much attention has been paid on forming processes of applicable two-layer metal sheets by several researchers. Due to different mechanical properties of base materials and key role of failure analysis of these laminated sheets, formability of two-layer sheets is of great interest by researchers. Parsa et al. [2] investigated the effect of thickness ratio and layers arrangement on the achievable drawing ratio in the deep drawing of aluminum/stainless steel two-layer sheets numerically and experimentally. Results showed that the aluminum to steel thickness ratio of 1/3 can result in a maximum drawing ratio. Formability of aluminum/copper two-layer sheets fabricated using the roll bonding process at different thickness ratios was studied by Tseng et al. [3] through finite element (FE) simulation and experiment. Because of residual stresses induced in the laminated sheet by the rolling process, it was reported that the formability of monolithic sheets is higher than that of two-layer sheets. Morovvati et al. [4] showed that the necessary blank holder force to avoid wrinkling in the conventional deep drawing of the aluminum/steel two-layer sheet prepared by adhesive bonding is lower and higher than that for a monolithic sheet of the base material with higher and lower strength, respectively. Jalali et al. [5] studied the effect of mechanical properties of base materials on formability of A1100/St13 two-layer sheets. The proposed theoretical model demonstrated that the forming limit diagram of the two-layer sheet is between the one of the constituent materials. Using experimental and numerical

* Corresponding author at: Mechanical Engineering Department, College of Engineering, University of Tehran, North Kargar Ave., PO Box 11155-4563, Tehran, Iran. Tel.: +98 6111 2768.
E-mail address: s_bagherzadeh@ut.ac.ir (S. Bagherzadeh).

http://dx.doi.org/10.1016/j.jmapro.2015.03.004

investigations on the deep drawing of aluminum/copper two-layer sheets, Atrian and Saniee [6] demonstrated that the layers arrangement can significantly affect the final part characteristics. Maleki et al. [7] studied the bonding strength and the critical thickness reduction in the rolling process of aluminum/steel two-layer sheets by using the analytical, numerical, and experimental approaches. They reported that the bonding strength and the critical reduction can be considerably affected by the yield strength and initial thickness of layers. The significance of adhesive bonding properties for the formability of steel two-layer sheets was researched by Satheeshkumar and Narayanan [8]. Based on experimental tensile tests, they concluded that by increasing the ratio of hardener to resin, the formability increases. Also, implementing an adhesive layer with a specified thickness between the two base layers can result in an improved longitudinal elongation when compared to a monolithic sheet or a two-layer sheet without any adhesive layer.

In previous researches, investigation on formability of sheets by making them as laminated sheets in the traditional forming processes like conventional deep drawing have been considered. Besides the conventional techniques, the sheet hydroforming process itself lead to an improvement in the formability of the sheet metal. Also, application of hydroforming process with high fluid pressure makes sure that sheet and punch contacts together during forming process tightly. Therefore, sheet hydroforming processes can be utilized to form multi-layer sheets with limited formability sheets more effective. In recent years, different sheet hydroforming methods have been extensively developed on forming of monolithic sheets and have been studied by using experimental and analytical approaches. Among them, hydro-mechanical deep drawing (HMDD) is one of the most widely used processes. In the HMDD process, as the punch moves against the pressurized fluid beneath the sheet, the blank is deformed to conform to the punch geometry. Fig. 1 schematically illustrates the HMDD process with its hydraulic circuit.

Lang et al. [9] conducted some experiments to investigate the process window in the one-layer HMDD process assisted by radial pressure at the flange edge. They found that by increasing the drawing ratio, the process windows for the pre-bulging pressure, the gap between the blank holder and the die, and the pre-bulging height become narrower. Fazli and Dariani [10] employed FE simulations based on the shell formulation to establish safe working zones for the fluid pressure vs. the drawing ratio in the HMDD of axisymmetric aluminum cups under the assumption of a uniform chamber pressure. They showed that it will be possible to reach higher drawing ratios in the HMDD process than in the conventional deep drawing if proper die radius, initial chamber pressure, and friction condition are adopted. In a similar work by Azodi et al. [11], using a tensile instability criterion under the plane strain assumption it was analytically shown that as the drawing ratio and the punch corner radius increase the critical fluid pressure decreases. Choi et al. [12] presented an analytical model capable of predicting wrinkling, fracture, and floating condition of the one-layer sheet metal in the warm HMDD process of axisymmetric parts and obtained the process window for the three effective parameters including the fluid pressure, the blank holder force, and the punch speed at a specified working temperature. The safe working zone in the HMDD of square cups was studied by Rahmani et al. [13] through FE modeling. They concluded that increasing the friction between the blank and the punch results in a wider working zone while decreasing the friction between the sheet and the blank holder has a reverse effect. Also, a higher drawing ratio can be achieved by using a larger radius of the punch corner.

Unlike the above mentioned work mainly focused on the hydroforming of monolithic sheets, Lang et al. [14] conducted numerical and experimental investigations on the hydroforming of multi-layer metal sheets consisting of a very thin aluminum layer in the middle and two steel sheets on both sides of that layer. Effects of layers arrangement and anisotropic properties of the two outer layers on the formability of the thin aluminum layer were studied. It was shown that the formability of the thin aluminum layer can be improved further as higher friction coefficients are considered between layers. To enhance the limited formability of the titanium alloy sheet, Tseng et al. [15] implemented the sheet hydroforming process for manufacturing a battery housing made of a titanium/aluminum two-layer sheet. Recently, instability of two-layer metal sheets in the HMDD process has been analyzed by Bagherzadeh et al. [16]. They predicted forming force and maximum fluid pressure as both experimentally and theoretically. The effect friction, layers arrangement and layers thickness ratio on the maximum critical pressure was assessed. Results showed that the analytical model is capable for calculating the maximum fluid pressure but cannot predict the entire safe working zone for the fluid pressure as well as formability, strain and thickness distribution of layers accurately.

In this research, a 3D finite element model was developed for accurate simulating the HMDD process of AL/St bimetallic sheet using commercial code Abaqus with dynamic explicit method. Unlike the previous researches considering a constant pressure on blank surface in the HMDD of monolithic sheets, a non-uniform fluid pressure model varying with time is incorporated into the Abaqus software as user-defined subroutine. The key parameters in sheet hydroforming such as entire process window (fluid pressure working zone), forming force, strain and thickness distribution of layers and forming limit diagram (LDR) predicted for HMDD process of laminated AL/St sheet. The experimentally validated FE model is used for studying the effect of layers arrangement on process parameters.

2. Experiments

2.1. Laminated sheets

Regarding wide industrial applications of aluminum/steel laminated sheets, in this research, two-layer sheets of low carbon steel st13 and aluminum alloy AA1050-O are considered. The selected sheet metals profit from the strength and formability of the steel sheet as well as the corrosion resistance, low density, and electrical conductivity of the aluminum sheet. Aluminum/steel two-layer sheets of 1.1 mm thickness with different combinations of the base sheet metals thickness were laminated by a two-component polyurethane base adhesive using binding method as described in [16]. The mechanical properties of the base sheet metals were determined according to ASTM E8-M standard along the rolling directions of 0°, 45°, and 90°, as depicted in Table 1.

Table 1
Mechanical properties of the base materials.

Properties	Low carbon steel (St13)	Aluminum (AA1050-O)
Thickness, t (mm)	0.4	0.7
Young modulus, E (MPa)	210,000	70,000
Yield strength, Y_0 (MPa)	152	35
Tensile strength, Y_S (MPa)	282	75
Strain hardening exponent, n	0.29	0.275
Hardening coeff., K (MPa)	496	112
Lankford anisotropy coefficients		
r_0	0.97	0.42
r_{45}	1.05	0.60
r_{90}	1.42	1.33

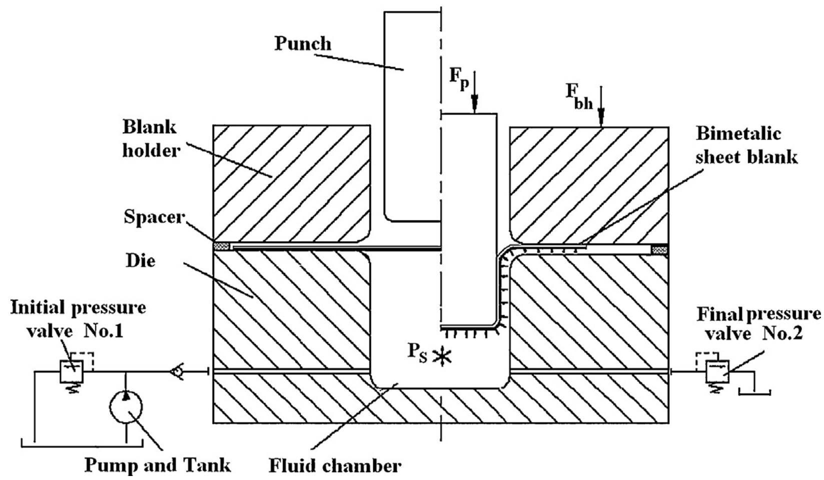

Fig. 1. Schematic illustration of the HMDD process.

2.2. Experimental equipment

Fig. 2 shows the utilized die set in the HMDD of cylindrical cups. The punch diameter, the clearance between the punch and the die, the inner diameter of the blank holder, and the corner radius of both the punch and the die are respectively equal to 40 mm, 2 mm, 41 mm, and 6.5 mm. A fixed gap system with 1.2 mm gap between the blank holder and the die was set by using three stiff spacers.

All experiments were carried out on a 50-ton hydraulic press. In these tests, firstly, the fluid chamber was fully filled with the hydraulic oil. Regarding the design of the experiments, a two-layer sheet was then placed on the die face based on the corresponding lay-up. To start forming operation according to the hydraulic diagram shown in Fig. 2(b), the initial pressure valve was located in the open state and the pre-bulging pressure was set to 20 bar. After pre-bulging, the initial pressure valve was closed and the pressure of the fluid chamber was controlled using the final pressure control valve. By adjusting a final pressure and with the punch progression to a desired depth at a constant speed of 2 mm/s, the HMDD was completed. In-plane strains induced in deformed parts were

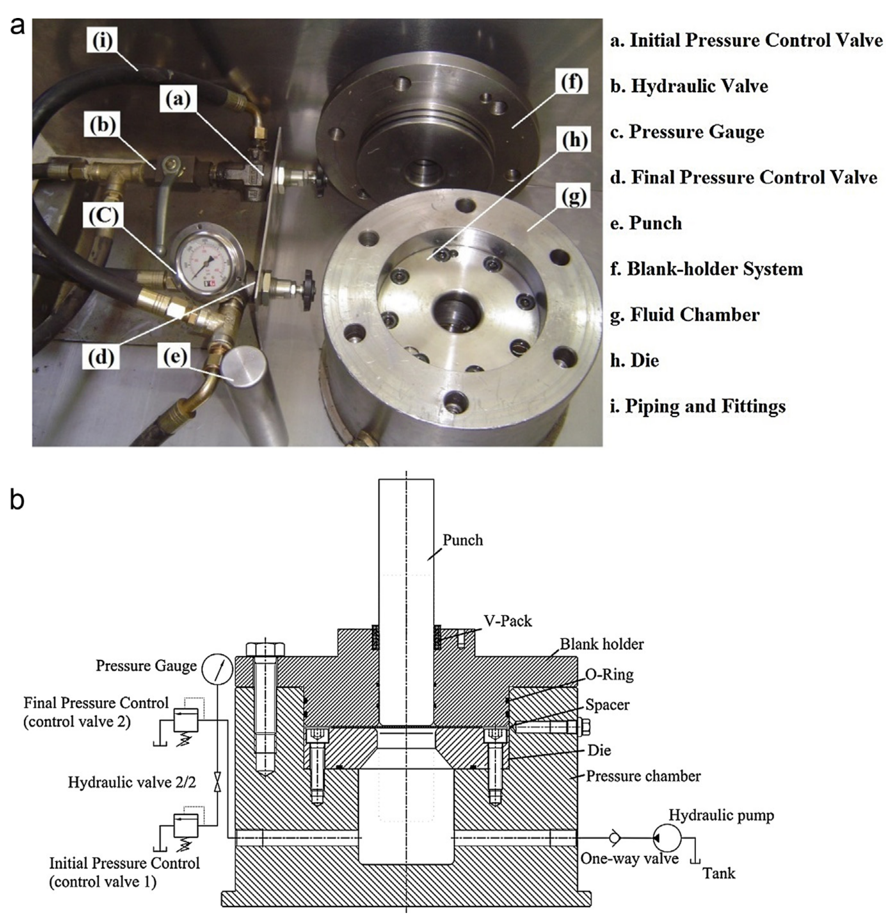

Fig. 2. (a) Experimental equipment of the HMDD process, (b) schematic of the utilized hydraulic circuit.

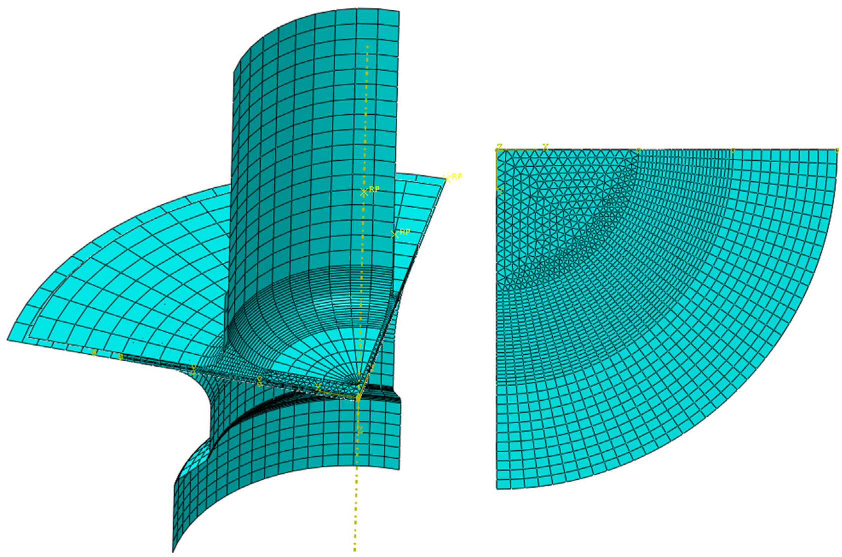

Fig. 3. FE model of the HMDD process.

measured using a grid pattern of circles with 4 mm diameter etched previously on initial blanks.

3. Finite element simulation

3.1. Modeling of the process

The commercial FE code Abaqus/Explicit was implemented to simulate the HMDD of two-layer metal sheets. To incorporate the effect of the material anisotropy and by considering the symmetry of the process, a 3D elasto-plastic model of the process consisting of only one quarter of the sheet and the die set was established as illustrated by Fig. 3. Symmetry boundary conditions were assigned to the edges of the model. The laminated sheet was split up into the corresponding two layers using the partitioning tool such that each layer has its own mechanical properties. The sheet was considered as a deformable body and discretized into 3078 elements of C3D8R and C3D4 type. The die components were modeled using rigid surface elements R3D4.

The anisotropic behavior of the material was taken into account using Hill's quadratic yield criterion as follows:

$$f(\sigma) = \sqrt{F(\sigma_{22}-\sigma_{33})^2 + G(\sigma_{33}-\sigma_{11})^2 + H(\sigma_{11}-\sigma_{22})^2 + 2L\sigma_{23}{}^2 + 2M\sigma_{31}{}^2 + 2N\sigma_{12}{}^2} \quad (1)$$

where σ_{ij} is the stress component and F, G, H, L, M, and N are the material parameters defined as [17]:

$$F = \frac{1}{2}\left(\frac{1}{R_{22}{}^2} + \frac{1}{R_{33}{}^2} - \frac{1}{R_{11}{}^2}\right), \quad G = \frac{1}{2}\left(\frac{1}{R_{33}{}^2} + \frac{1}{R_{11}{}^2} - \frac{1}{R_{22}{}^2}\right),$$
$$H = \frac{1}{2}\left(\frac{1}{R_{11}{}^2} + \frac{1}{R_{22}{}^2} - \frac{1}{R_{33}{}^2}\right), \quad L = \frac{3}{2R_{23}{}^2},$$
$$M = \frac{3}{2R_{13}{}^2}, \quad N = \frac{3}{2R_{12}{}^2} \quad (2)$$

In which R_{ij} is the anisotropic yield stress ratio. By assuming $R_{11} = 1$, R_{ij} can be written as:

$$R_{22} = \sqrt{\frac{r_{90}(r_0+1)}{r_0(r_{90}+1)}}, \quad R_{33} = \sqrt{\frac{r_{90}(r_0+1)}{(r_0+r_{90})}},$$
$$R_{12} = \sqrt{\frac{3(r_0+1)r_{90}}{(2r_{45}+1)(r_0+r_{90})}} \quad (3)$$

Here, it is convenient to assume that $R_{13} = R_{23} = 1$. Hence, R_{ij} can be calculated using the Lankford coefficients obtained for the steel and aluminum sheets.

The Coulomb friction was implemented to define contact interfaces between surfaces. As the sheet is supported by a fluid film at the lower layer/die contact interface and due to the possibility of the fluid leakage into the gap between the upper layer and the blank holder, the friction coefficients at the lower layer/die, upper layer/blank holder, and upper layer/punch face interfaces were assumed to be 0.05, 0.08, and 0.1, respectively, based on the previous researches in this field [10,22,23]. An appropriate time scaling scheme in which the ratio of the kinetic energy to the internal energy is negligible was utilized to reduce the simulation time artificially.

3.2. Oil pressure distribution model

The fluid pressure at the pre-bulging stage was gradually applied to the sheet with a uniform distribution over the entire sheet surface. The variation of the oil pressure till the prescribed final pressure during the deep drawing stage is one of the most effective parameters on achieving a successful part. It should be noted that the distribution of the fluid pressure over the sheet is not uniform in the HMDD process [18,19]. To simulate the process more accurately, the non-uniform distribution of the fluid chamber pressure onto the sheet surface and its variation with time were considered based on the mathematical model proposed by (Jensen et al. [18], Lang et al. [19]) and incorporated into the FE model by an appropriate subroutine *VDLOAD developed in Visual Fortran software and implemented in Abaqus. Accordingly, in each forming time step (t), as shown in Fig. 4(a) the blank geometry is partitioned by developed code into the flange region (with non-uniform oil pressure with respect to "x") and the zone consisting of curved section, wall

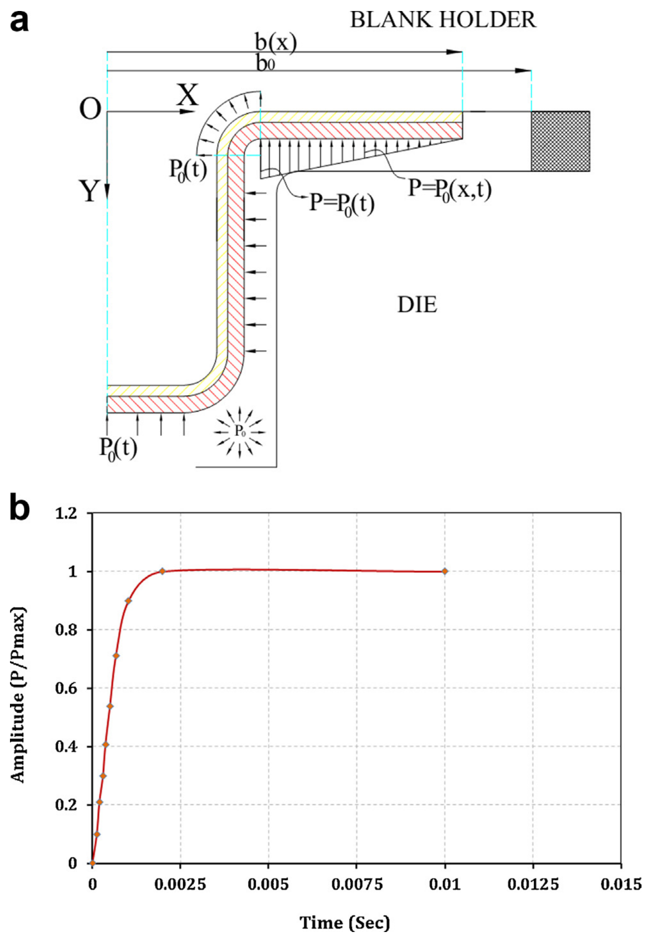

Fig. 4. (a) Schematic description of oil pressure distribution on blank, (b) variation of normalized pressure with time during forming progress.

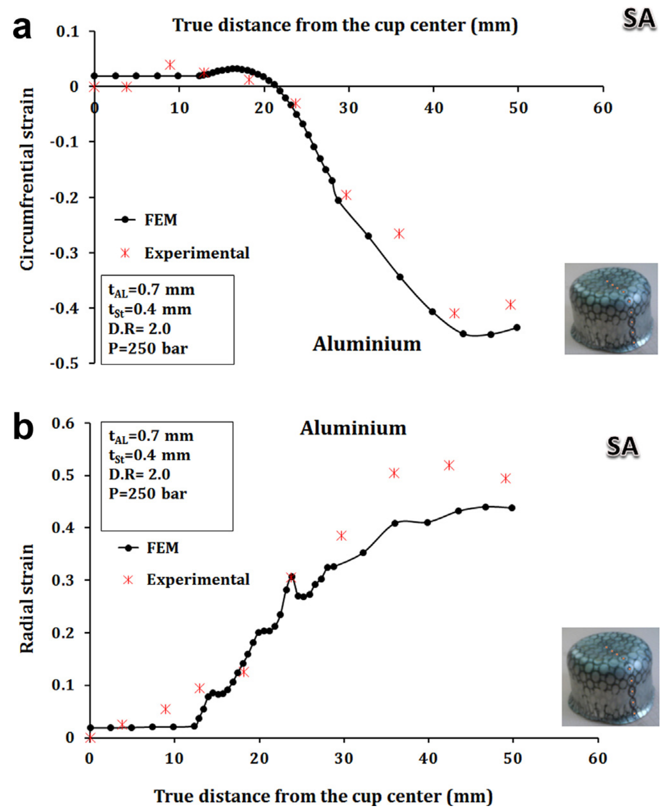

Fig. 6. Comparison of measured and predicted strain distribution in the aluminum layer of the cup shown in Fig. 6. (a) Radial strain and (b) circumferential strain.

and the bottom of the blank (with uniform pressure with respect to "x"). In addition, during forming progress, a non-uniform linear pressure with respect to time (t) is applied onto the blank surface points till oil pressure reaches to maximum adjusted pressure. Fig. 4(b) depicts oil pressure path normalized to maximum adjusted pressure ($P(t)/P_{max}$) with respect to process time (scale down) measured during experiments from pressure gauge in good accordance to oil pressure path reported in the literature [18]. This presented pressure path was utilized in developed FE model using amplitude toolset.

3.3. *Failure criterion*

Different failure criteria can be used in FE simulation. The applicability of conventional forming limit diagrams (FLD) to predict forming failure is somewhat restricted as 3D solid elements are used compared to shell elements in the FE modeling [20]. This paper deals with the overall success prediction of the forming process rather than the exact prediction of the failure onset. Here, the equivalent plastic strain history of elements along radial paths in

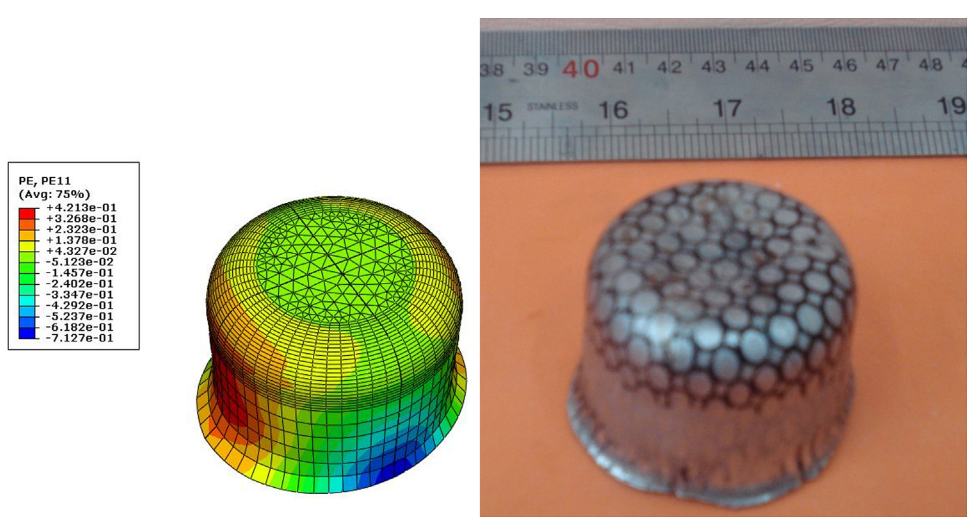

Fig. 5. Hydro-mechanical deep drawn cup with the SA lay-up and St 0.4 mm/Al 0.7 mm thickness combination formed at the drawing ratio of 2 and by the pressure of 250 bar.

the middle section of the model was evaluated after each simulation. A sudden change in the strain gradient leading to an excessive increase in the equivalent plastic strain of an element compared to the strain trend of other elements was regarded as the forming failure initiating in that element. The same approach has been successfully implemented to obtain forming limit diagrams of sheet metals [21].

4. Results and discussion

In the following results, the aluminum and steel layers of the laminated sheet metal are respectively denoted by A (or Al) and S (or St). The lay-up in which the aluminum layer is in contact with the punch while the steel layer is on the side of the fluid chamber is denoted with “AS”, and vice versa, the “SA” lay-up can be defined. The thickness of the two-layer sheet is equal to 1.1 mm.

4.1. Validation of the FE model

To validate the FE model, the HMDD of the aluminum/steel two-layer sheet at different drawing ratios and pressures of the fluid chamber was simulated and compared with experiments considering an initial pressure of 20 bar for the pre-bulging stage. Fig. 5 shows the experimental and simulated configurations of a cylindrical cup with SA lay-up and the thickness combination of 0.4 mm and 0.7 mm for the steel and aluminum layers, respectively.

Radial and circumferential strains corresponding to the outer (aluminum) layer of the mentioned part obtained using the FE model and the experiments are shown in Fig. 6. A reasonably good agreement can be seen between predicted and measured results. The differences between experimental and computed results at the radii far away from the center of the part (true distance from cup center between 36 mm up to 50 mm) are rather higher than those at the part center that shows the maximum error 11% and error 19% both in $x = 35.9$ mm for circumferential and radial strains respectively. It can be attributed to accuracy of measuring method and the negligible wrinkling occurred in the flange region.

Fig. 7(a) compares the forming force curve during HMDD process for a formed cup with the AS lay-up and the thickness combination of 0.4 mm and 0.7 mm for the steel and aluminum layers, respectively. As shown in this figure, the overall trend of forming force

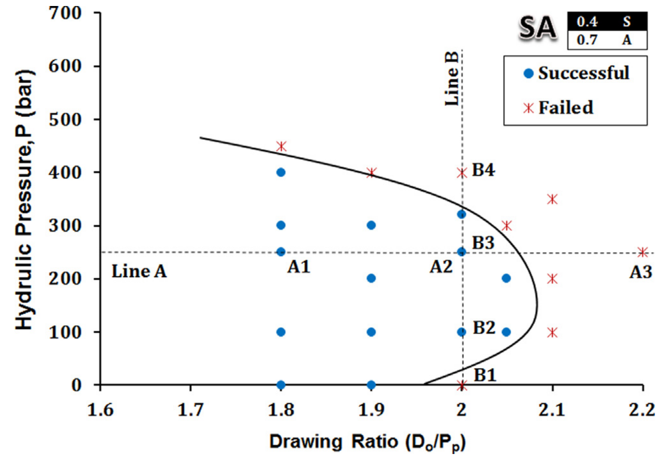

Fig. 8. Predicted process window for the HMDD of a two-layer sheet with the indicated lay-up and the thickness combination.

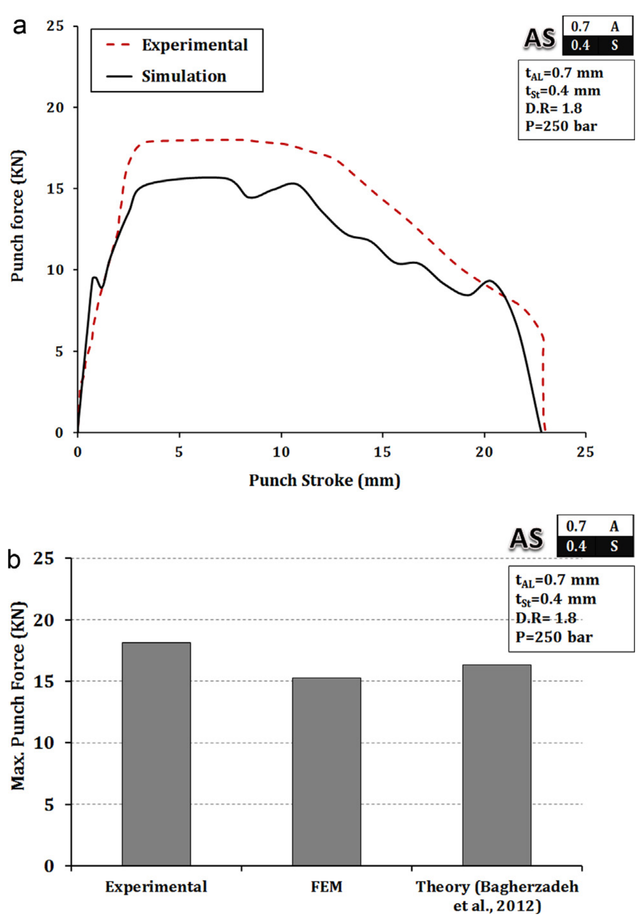

Fig. 7. Comparison of (a) forming force curve calculated from FE model and experiments, (b) the maximum forming force obtained using the experiment, the FE model, and the theoretical approach ([16]).

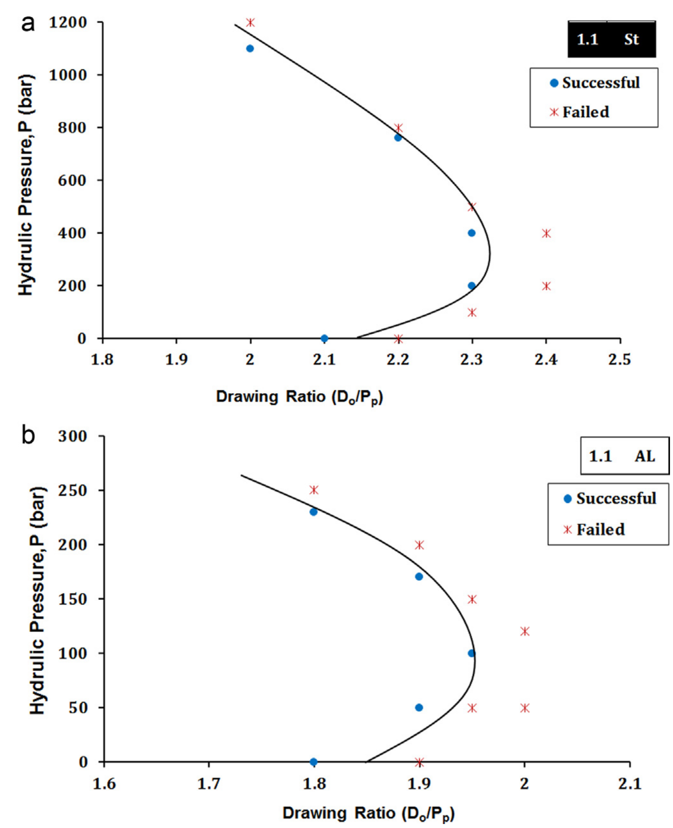

Fig. 9. Predicted process windows for the monolithic sheets of (a) steel and (b) aluminum.

curve determined by FE model and measured from machine load-cell was in good agreement although the upper level of forming force indicates error. Fig. 7(b) compares the maximum forming forces obtained using the experiment, the FE model, and the theoretical approach presented by (Bagherzadeh et al. [16]) in same cup which was formed at the drawing ratio of 1.8 and adjusted maximum fluid pressure of 250 bar. Due to the deviation between the real and implemented pressure path in the FE model and the wrinkling occurred in the flange region, the measured experimental maximum force was higher than the computed one. In addition, the FE result predicted the maximum force slightly lower than theoretical approach (as calculated by [16]) which can be explained with considering assumptions in the theoretical method such as the plane stress condition.

4.2. *Prediction of process windows*

The working zone of the fluid pressure and consequently the resulting blank holding force are some of the critical parameters affecting the success of the HMDD process. Using the developed FE model, the success and the failure of the HMDD of two-layer metal sheets with different arrangements at various drawing ratios and fluid pressures have been predicted based on the aforementioned failure criterion. The pre-bulging pressure was constant equal to 20 bar. By plotting a curve specifying the boundary between successful and unsuccessful forming conditions, a process window indicating the safe zone for the fluid pressure vs. the drawing ratio can be established. The process window for the AS lay-up with the thickness combination of 0.4 mm and 0.7 mm for the steel and aluminum layers, respectively, is illustrated in Fig. 8.

It can be observed from Fig. 8 that as the drawing ratio increases, the safe working zone for the critical fluid pressure becomes narrower. Fig. 8 also shows that in the HMDD process the maximum drawing ratio ensuring a successful part forming and known as limiting drawing ratio (LDR) is higher than the one in the conventional deep drawing which is represented by the cases on the *x*-axis of Fig. 8 at which the fluid pressure is equal to zero. It means that the HMDD process provides the higher formability of two-layer sheets than the conventional deep drawing. The process windows for the HMDD of the monolithic sheets of aluminum and steel with the same thickness as the two-layer sheet are illustrated in Fig. 9. It is obvious that the trend of the critical fluid pressure with the drawing ratio is the same for the two-layer and monolithic sheet.

Fig. 10 demonstrates the distribution of equivalent plastic strains predicted using the FE model in the samples denoted as A1–A3 and B1–B4 by Fig. 8. The samples A1–A3 have been deep

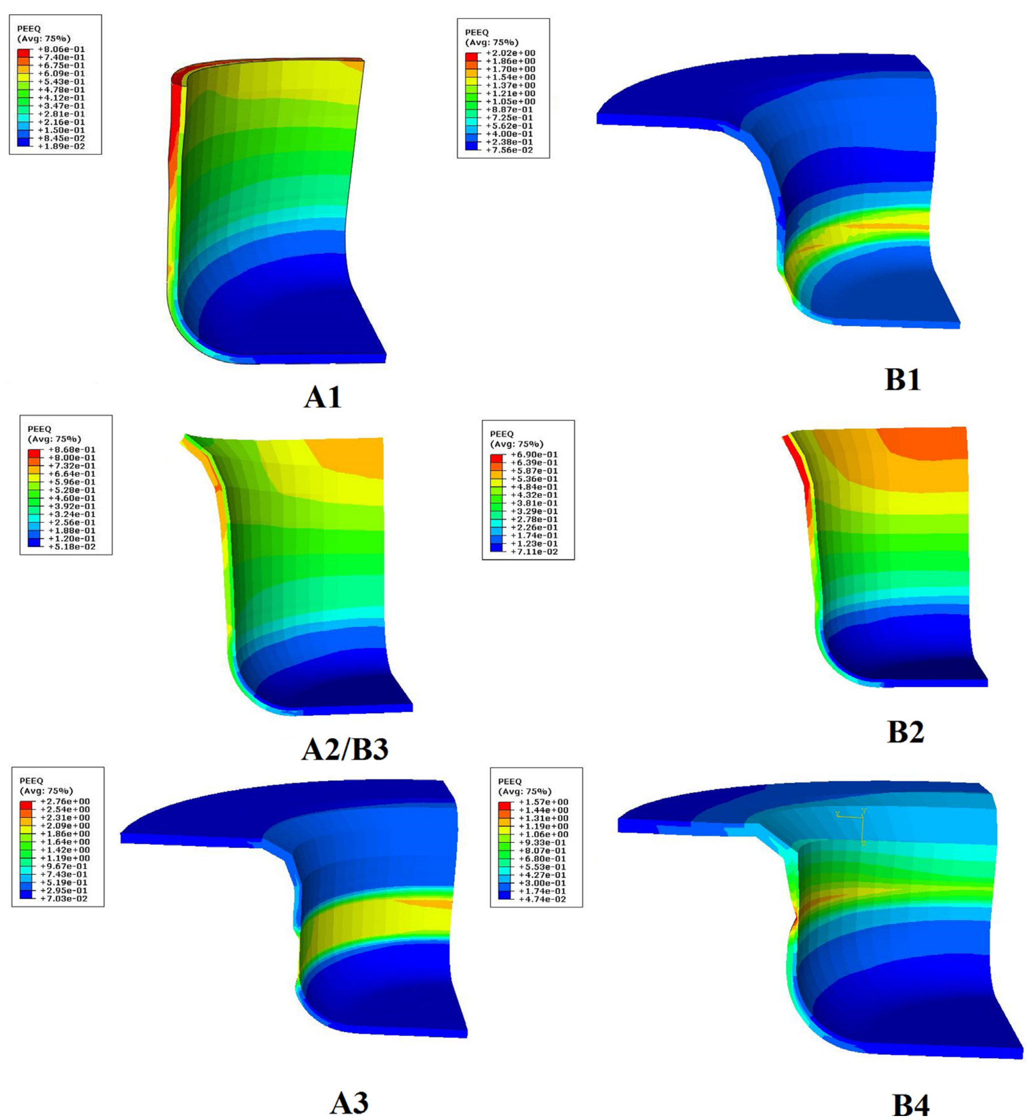

Fig. 10. Simulated configuration of the samples mentioned in Fig. 8 for the two-layer sheets with the SA lay-up and the thickness combination of St 0.4 mm/Al 0.7 mm.

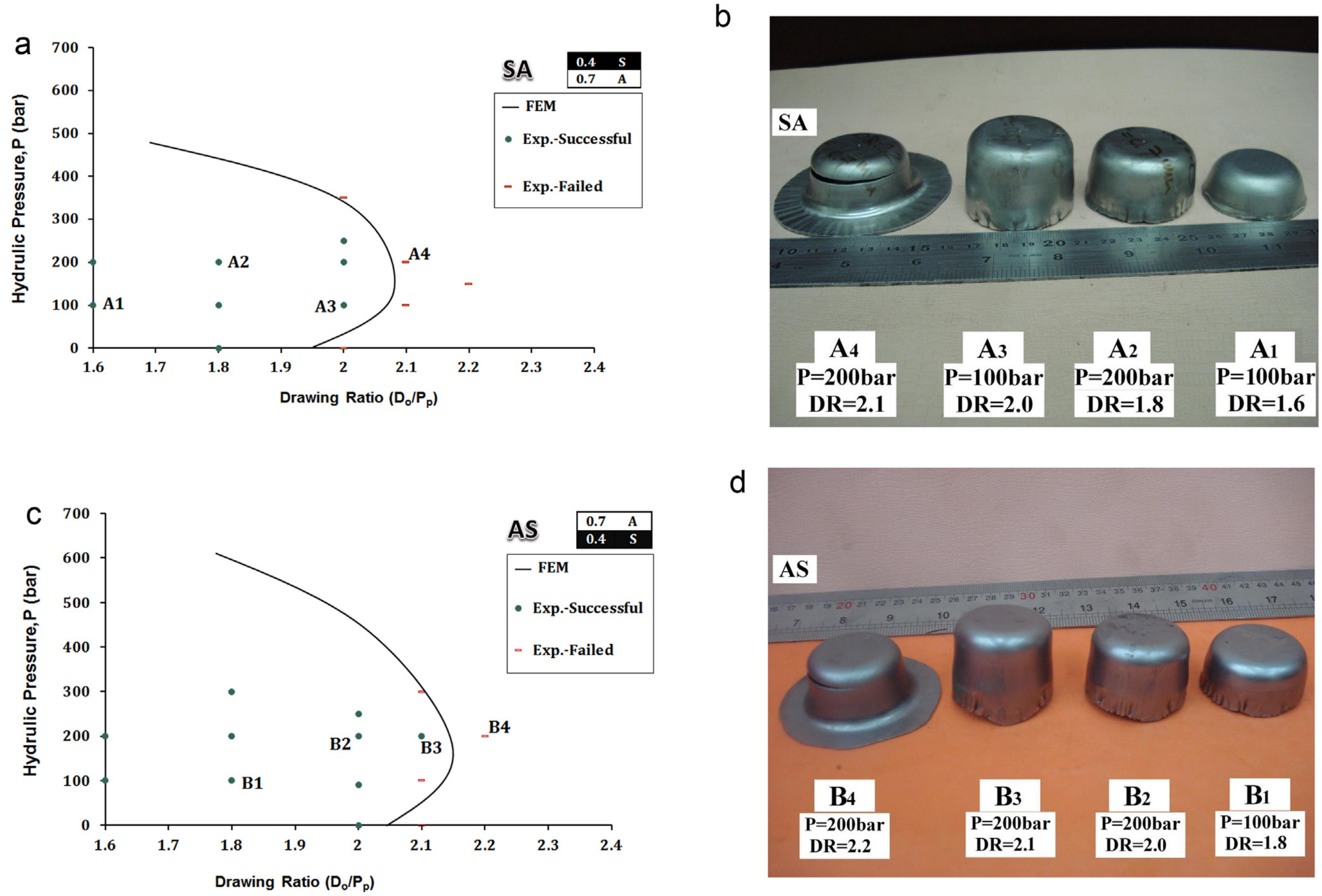

Fig. 11. Assessment of the predicted process window with the experimental results for (a), (b) S/A lay-up and (c, d) A/S lay-up.

drawn by the fluid pressure of 250 bar at various drawing ratios and the samples B1–B4 have been formed with the drawing ratio of 2 under different pressures of the fluid chamber. The sample B1 formed without the fluid pressure identically represents a conventionally deep drawn part. As depicted in Fig. 10, like the deep drawing process, the excessive thinning in the sample B1 which leads to a part failure is occurred at the punch corner due to the increase of friction and tension and the contact between the sheet and the die corner as a result of the non-floating condition of the blank. Compared to the sample B1, the sample A3 deep drawn by the drawing ratio of 2.2 under the 250 bar fluid pressure shows a different thinning zone on its wall between the die and punch corner. A rather high fluid pressure of 400 bar has been applied to form the sample B4 at the drawing ratio of 2 resulting in an excessive thinning closer to the die corner which can be related to the extreme contact between the sheet and the punch and also the floating state of the blank with a low radius of the curvature at the die corner. So, it can be stated that in the HMDD of the laminated sheets, as the fluid pressure increases the failure region on the wall moves from the punch corner toward the die corner.

In order to assess the accuracy of process windows obtained using FE simulations, the successful and unsuccessful forming of some samples inside and outside the predicted working zone have been experimentally verified. Table 2 summarizes some of the experiments.

As it can be seen, at the drawing ratio of 2.1 and the fluid pressure of 200 bar the SA lay-up has been collapsed while the AS lay-up with the same thickness combination has been successfully formed. Fig. 11 illustrates the simulated process windows for the both possible SA and AS lay-ups of St 0.4 mm/Al 0.7 mm thickness combination with corresponding experiment results. The experimental results confirm and validate the predicted safe working region well.

Table 2
Some of experiments to verify predicted process windows.

Sheet Lay-up	Marks	Drawing ratio	Pressure (bar)	Forming condition
"S/A" lay-up	Case "A1"	1.6	100	Success
	Case "A2"	1.8	200	Success
	Case "A3"	2.0	100	Success
	Case "A4"	2.1	200	Failed
"A/S" lay-up	Case "B1"	1.8	100	Success
	Case "B2"	2.0	200	Success
	Case "B3"	2.1	200	Success
	Case "B4"	2.2	200	Failed

4.3. Parameters study

4.3.1. Effect of lay-up on process window

According to simulations results, it is revealed that the safe working zone for the fluid pressure can be affected by the lay-up of the two-layer sheet. The effect of the lay-up on the process window at different thickness combinations of the aluminum and steel sheets obtained by using the FE model is demonstrated in Fig. 12. By utilizing the AS lay-up rather than the SA one for all of the investigated thickness combinations, it is possible to achieve a wider working zone for the fluid pressure ensuring a successful drawing. This is mainly due to the less thinning and protection of the weaker material with the lower formability, i.e. aluminum layer, at likely

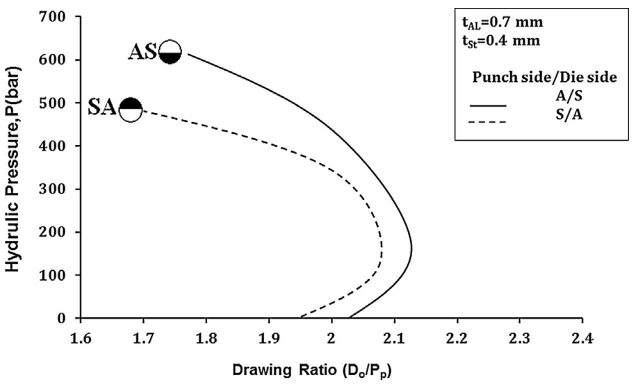

Fig. 12. Effect of lay-up on the process window predicted using FE simulation.

failure zones in the AS lay-up, which is confirmed by the analysis of the thickness distribution of the two layers. Furthermore, regarding Fig. 12, the difference between safe working zones calculated for the two lay-ups increases as the drawing ratio decreases.

4.3.2. Effect of thickness combination on process window

Fig. 13 indicates variations of the safe working zone in the HMDD process by changing the thickness combination at the both SA and AS lay-ups. The thickness combination can vary from the monolithic sheet of aluminum to the steel one. According to Fig. 13 for the both lay-ups, as the thickness of the material with the higher strength, i.e. steel layer increases the working zone for the fluid pressure becomes wider. The figure also shows that for the wider working zone, the AS lay-up should be implemented in HMDD process of Al/St bimetallic sheets.

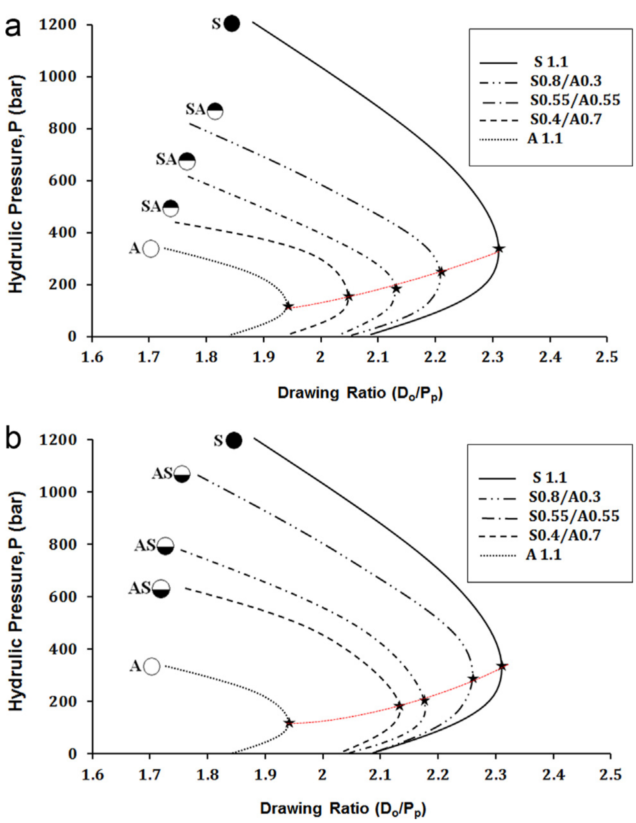

Fig. 13. Effect of thickness combination on the process window predicted using FE simulation for (a) the SA and (b) the AS lay-up.

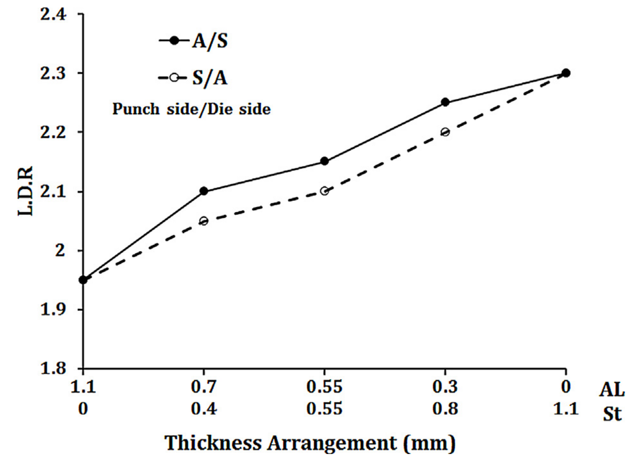

Fig. 14. Predicted LDR at various thickness combinations and lay-ups.

4.3.3. Effect of layers arrangement on LDR

As shown in previous figures, the process window for the fluid pressure vs. the drawing ratio is defined by a nose-like curve. The nose indicates the LDR for a successful forming at a specified arrangement of the two-layer sheet. Fig. 14 shows the predicted LDR for the both lay-ups at different thickness combinations including the single layer sheets of aluminum and steel. By increasing the thickness of the layer with the higher formability, i.e. steel layer, the LDR of the two-layer sheet increases. Hence, the maximum

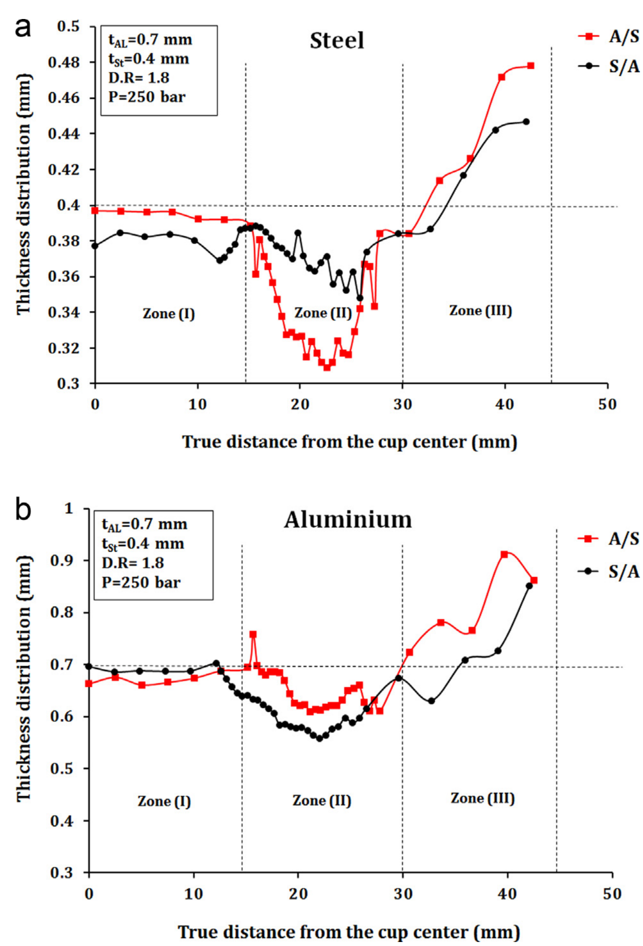

Fig. 15. Comparison of the thickness distribution of (a) the steel layer and (b) the aluminum layer in the SA and AS lay-ups obtained using the FE model.

LDR belongs to the monolithic sheet of steel with the thickness of 1.1 mm. It is noticeable that by implementing a two-layer sheet in which the thickness of the steel layer is smaller than 1.1 mm, a LDR between the ones of the monolithic sheets of base materials can be achieved as well as a weight reduction in the laminated sheet. As it can be seen, by the lay-up in which the layer with a lower formability is in contact with the punch and the layer with a higher strength is on the die side, a slightly higher LDR can be attained leading to form a deeper part.

4.3.4. *Effect of layers arrangement on thickness distribution*

Fig. 15 compares the thickness distribution of each layer in the both lay-ups. Based on the figure, regardless of the lay-up, the outer layer has the minimum thickness. As shown in Fig. 15(a), the thickness of the steel layer at the bottom of the part, i.e. zone I, in the AS lay-up is approximately constant while it is slightly reduced in the SA lay-up. This is due to the direct contact of the steel layer with the punch in the SA lay-up and a higher friction coefficient in this interface. At zone II including the punch corner and the cup wall, the sheet experiences more thickness reduction in the AS lay-up than in the SA one. The fracture is likely to occur in this region as previously reported for the conventional deep drawing (near the punch corner) and HMDD processes (the upper region of the wall). Compared to the SA lay-up, more thickening which can result in wrinkling, is happened in the AS lay-up at the flange region of the steel layer, i.e. zone III. Regarding Fig. 15(b), a reverse trend in the thickness distribution with respect to the one described above is observed for the aluminum layer. Unlike the steel layer, the aluminum layer shows a less thinning at the AS lay-up than the SA lay-up in zone II. Hence, to avoid the tearing in the weaker material, particularly for a two-layer sheet with a thin layer of aluminum, it is appropriate to use the AS lay-up.

5. Conclusions

In this research, a 3D FE model of the HMDD of aluminum/steel two-layer sheets was developed to predict the key process parameters ensuring a successful forming for fluid pressure vs. drawing ratio. By comparing simulated results with experimental ones, a reasonable good agreement confirming the capability of the FE model to predict the process parameters was observed. Furthermore, effect of thickness combination and lay-up of the two layer sheet on the process window, formability of layers and the thickness distribution were investigated through FE simulations. The main conclusions can be drawn as follows:

- The HMDD process with proper fluid pressure improves formability and LDR in forming of Al/St bimetallic sheets than conventional deep drawing. Applying hydraulic pressure under blank during forming moves failure region from the punch corner zone toward the die corner zone based on applied pressure value.
- At a specified lay-up and thickness combination, by increasing the drawing ratio the critical pressure decreases and consequently the upper limit of safe working zone for the fluid pressure becomes narrower and also applying fluid pressure increases limiting drawing ratio for formed cup than conventional deep drawing, which results in a nose-like curve for the process window.
- The process window and the safe working zone for the fluid pressure in the AS lay-up is wider as compared to the SA lay-up. Higher drawing ratios and LDRs can be achieved by implementing the AS lay-up than the SA lay-up.
- As the thickness of the layer with a higher strength increases, a broader working zone is attained. Due to the more thinning of the aluminum layer occurred in the SA lay-up at the wall region, it can be suggested to use the AS lay-up instead of the SA one to avoid tearing in the layer with a lower formability.

As future work, using developed FE model and proposed theoretical approach formerly, the mechanics of laminated sheet deformation in HMDD process accompanied with stress and strain components analysis of layers will be analyzed and the failure modes will be discussed.

References

[1] Bykov AA. Bimetal production and applications. Steel Trans 2011;41:778–86.
[2] Parsa MH, Yamaguchi K, Takakura N. Redrawing analysis of aluminum-stainless-steel laminated sheet using FEM simulations and experiments. Int J Mech Sci 2001;43:2331–47.
[3] Tseng HC, Hung C, Huang CC. An analysis of the formability of aluminum/copper clad metals with different thicknesses by the finite element method and experiment. Int J Adv Manuf Technol 2010;49:1029–36.
[4] Morovvati MR, Fatemi A, Sadighi M. Experimental and finite element investigation on wrinkling of circular single layer and two-layer sheet metals in deep drawing process. Int J Adv Manuf Technol 2011;54:113–21.
[5] Jalali Aghchai A, Shakeri M, Mollaei Dariani B. Influences of material properties of components on formability of two-layer metallic sheets. Int J Adv Manuf Technol 2013;66:809–23.
[6] Atrian A, Saniee FF. Deep drawing process of steel/brass laminated sheets. Composite B 2013;47:75–81.
[7] Maleki H, Bagherzadeh S, Mollaei Dariani B, Abrinia K. Analysis of bonding behavior and critical reduction of two-layer strips in clad cold rolling process. J Mater Eng Perform 2013;22:917–25.
[8] Satheeshkumar V, Narayanan RG. Investigation on the influence of adhesive properties on the formability of adhesive-bonded steel sheets. Proc IMechE C: J Mech Eng Sci 2014;228:405–25.
[9] Lang L, Danckert J, Nielsen KB. Investigation into hydrodynamic deep drawing assisted by radial pressure. Part I: Experimental observations of the forming process of aluminum alloy. J Mater Process Technol 2004;148:119–31.
[10] Fazli A, Mollaei Dariani B. Parameter study of the axisymmetric hydromechanical deep drawing process. Proc IMechE B: J Eng Manuf 2006;220: 1937–44.
[11] Azodi HD, Naeini HM, Parsa MH, Liaghat GH. Analysis of rupture instability in the hydromechanical deep drawing of cylindrical cups. Int J Adv Manuf Technol 2008;39:734–43.
[12] Choi H, Koc M, Ni J. A study on the analytical modeling for warm hydro-mechanical deep drawing of lightweight materials. Int J Mach Tools Manuf 2007;47:1752–66.
[13] Rahmani F, Hashemi SJ, Naeini H, Azodi HD. Numerical and experimental study of the efficient parameters on hydromechanical deep drawing of square parts. J Mater Eng Perform 2013;22:338–44.
[14] Lang L, Danckert J, Nielsen KB. Multi-layer sheet hydroforming: experimental and numerical investigation into the very thin layer in the middle. J Mater Proc Technol 2005;170:524–35.
[15] Tseng HC, Wu ZC, Hung C, Lee MH, Huang CC. Investigation of optimum process parameters on the sheet hydroforming of titanium/aluminum clad metal for battery housing. In: 4th Int. Conf. on Tube Hydroforming. 2009.
[16] Bagherzadeh S, Mollaei Dariani B, Malekzadeh K. Theoretical study on hydro-mechanical deep drawing process of bimetallic sheets and experimental observations. J Mater Proc Technol 2012;212:1840–9.
[17] Abaqus analysis user's manual, version 6.10; 2010.
[18] Jensen MR, Olovsson L, Danckert J. Numerical model for the oil pressure distribution in the hydromechanical deep drawing process. J Mater Proc Technol 2000;103:74–9.
[19] Lang LH, Danckert J, Nielsen KB, Kang DC, Zhang SH. Key technologies of the simulation of the hydrodynamic deep drawing of irregular parts. J Mater Proc Technol 2004;150:40–7.
[20] Zhang C, Leotoing L, Zhao G, Guines D, Ragneau E. A comparative study of different necking criteria for numerical and experimental prediction of FLCs. J Mater Eng Perform 2011;20:1036–42.
[21] Mamusi H, Masoumi A, Hashemi R, Mahdavinejad R. A novel approach to the determination of forming limit diagrams for tailor-welded blanks. J Mater Eng Perform 2013;22:3210–21.
[22] Zhang SH, Jensen MR, Nielsen KB, Danckert J, Lang LH, Kang DC. Effect of anisotropy and prebulging on hydromechanical deep drawing of mild steel cups. J Mater Proc Technol 2003;142:544–50.
[23] Fazli A, Dariani BM. Theoretical and experimental analysis of the axisymmetric hydromechanical deep drawing process. Proc Inst Mech Eng B: J Eng Manuf 2006;220:1429–37.